



Investigations of structural modifications, physical and optical properties of lead boro-tellurite glasses doped with europium trioxide for possible optical switching applications

G. V. Jagadeesha GOWDA¹, G. V. Ashok REDDY², Bheemaiah ERAIAH³, Chinnappa Reddy DEVARAJA^{4,*}

¹ Department of Physics, BGS College of Engineering and Technology, Bengaluru-560086, Karnataka, India

² Department of Physics, Nitte Meenakshi Institute of Technology, Bengaluru-560064, Karnataka, India

³ Department of Physics, Bangalore University, Bengaluru 560056, India

⁴ Department of Physics, Manipal Institute of Technology Bengaluru, Manipal Academy of Higher Education, Manipal 576104, Karnataka, India

*Corresponding author e-mail: deva.drr@gmail.com

Received date:

18 January 2023

Revised date

7 April 2023

Accepted date:

7 April 2023

Keywords:

MAS-NMR;
Polaron radius;
UV-visible spectroscopy;
Urbach energy;
Optical basicity

Abstract

This manuscript intends to the structural modifications, and physical and optical properties of a set of heavy metal alkali boro-tellurite glasses doped with Eu_2O_3 . These glasses were produced by a conservative melt-quenching method. The existence of non-crystalline properties in the glasses was ascertained by X-ray diffraction analysis. The structural modifications were noticed by MAS-NMR spectroscopic investigation. Physical properties such as density, molar volume, oxygen packing density, average boron-boron separation, interionic distance, and polaron radius have been calculated by a suitable approach. The optical absorption studies were made through UV-visible absorption spectroscopy in the 350 nm to 800 nm wavelength range. The optical properties namely, optical energy bandgap, Urbach energy, optical basicity, electronegativity, and electric susceptibility, were also determined by using appropriate methods. The MAS-NMR spectroscopic experiments reveal that fewer BO_4 units are converted to BO_3 units and those NBOs are turned into bridging oxygen at a lower rate. The optical refractive index values and optical dielectric constant range from 2.241 to 2.358, and 5.0220 to 5.5601, respectively. The obtained energy band gap values ($E_{g(d)}$: 3.367 eV to 3.597 eV and $E_{g(ind)}$: 2.109 eV to 2.863 eV) and other significant optical parameters suggest that the investigated glasses are potential candidates for europium-doped fiber amplifier applications and possible optical switching applications.

1. Introduction

High refractive index, relatively high optical dielectric constant, strong transmittance near the IR region, and high third-order optical nonlinearities are all well-known physical and optical features of glasses containing heavy metal oxides [1-5]. Tellurium dioxide (TeO_2) is the one of the good conditional glass former, but it cannot cause form glass itself directly, therefore other supporting metal oxides such as PbO , WO_3 , La_2O_3 , Bi_2O_3 are required as glass modifiers to prepare boro-tellurite glasses. Moreover, to achieve a high refractive index, multicomponent oxide glasses incorporating PbO , WO_3 , La_2O_3 , TeO_2 , Bi_2O_3 , and Nb_2O_5 have recently been synthesized [2-8]. If the glasses have a refractive index that is higher than $n \sim 2$, coloration occurs, which is primarily driven by the optical absorption edge, which is placed near-visible wavelength rather than deep-UV wavelength. Furthermore, the transmittance spectra of glasses are generally reduced around the absorption edge, resulting in greyish and yellowish colors in high refractive index glasses. It has been demonstrated that the transmittance shortfall towards the absorption edge is caused not only by impurity contamination [2], but also by glass structure disorder

[3] or heavy metal cation valency changes [3-5]. The electronic resonance near the absorption edge improves the refractive index and optical nonlinearity significantly [5,6]. It has been observed that in glasses with a high refractive index, the blue-shifted absorption edge (wavelength less than 400 nm) and high transmittance in visible wavelength can be attained concurrently [2]. The optical nonlinearity of high refractive index features of various oxide glasses containing Pb, Bi, Te, and Chalcogenide glasses was investigated [4-11]. The bandgap energy (E_g) of boro tellurite glasses with different concentrations of Eu_2O_3 plays a crucial role in determining their switching performance. Several studies have investigated the effect of Eu_2O_3 concentration on the bandgap energy of boro tellurite glasses. It has been observed that the bandgap energy of boro tellurite glasses decreases with increasing Eu_2O_3 concentration. For instance, a study by El-Mallawany *et al.* [8] reported a decrease in the bandgap energy of boro tellurite glasses from 3.27 eV to 3.09 eV with increasing Eu_2O_3 concentration from 0 mol% to 0.8 mol%. These glasses have a high third-order nonlinear susceptibility of $\chi_3 \sim 10^{(-11)}$ esu, and a typical high refractive index of 1.9 to 2.5. The presence of the absorbance edge has an impact on the glasses optical nonlinearity, as a result, the stronger the optical

nonlinearity, the richer the coloration of the glasses. Because these glasses have a high transmittance in the near-infrared range, they can be employed as optical fibers in telecommunication wavelengths. Instead, the transmittance spectra near the absorption edge, particularly in high refractive index glasses, has been widely explored.

The effect of europium trioxide on the structural, physical, and optical aspects of alkali lead boro-tellurite glasses [LABT] is discussed in this paper. LABT has a rather sharp absorption edge, which is difficult to be noticed in traditional glasses with a high refractive index. The "Urbach Rule" [4,11-13] is used to study the structure of absorption spectra. Furthermore, B_2O_3 , TeO_2 , and PbO contents are likely to have a significantly high refractive index and strong optical nonlinearity. Electronic polarizability and optical basicity were used to examine the refractive index and related optical properties of the obtained glasses [2-4,7-9].

2. Experimental procedures

2.1 Preparation of glass

The Eu_2O_3 doped alkali lead boro-tellurite glasses possessing chemical composition $(70-y) B_2O_3-15TeO_2-10Na_2O-5PbO-y(Eu_2O_3)$, where y is considered as 0.0, 0.1, 0.2, 0.3, 0.4 and 0.5 mol%, were fabricated by usual melt-quenching technique [1,4,11,14]. Here onwards, the synthesized sets of glasses are termed LABT0, LABT1, LABT2, LABT3, LABT4, and LABT5. The chemicals that were procured from Sigma Aldrich have appeared in powder form and have high purity of 99.9%. The chemical powders are weighed by using digital chemical balance according to stoichiometry and transferred to agate mortar, and chemicals were appropriately stirred over 35 min to get a homogenous mixture. The achieved homogeneous mixture was then placed into porcelain crucibles. The crucibles with the chemical mixture were kept inside the electric muffle furnace for heating. The chemicals were heated at $1100^\circ C$ for 1.5 h. Furthermore, the molten substance is stirred regularly to get the homogeneity in samples. The molten substance was then dispensed and sandwiched between brass molds and pressed to each other. To achieve glasses, having no thermal stress in them, the synthesized glass substances were kept in a furnace for annealing at $360^\circ C$ for about 2 h. The obtained glasses as showed in figure were then taken in desired shape and size for appropriate characterizations.

2.2 X-Ray Diffraction (XRD)

Generally, the non-crystallinity studies were conducted on the prepared glass sample in powder form. The transparent glass samples were squashed by using a pestle and mortar to achieve fine and homogeneous powder samples and were then ground thoroughly with a plunger and grinder. The Bruker D8 Focus X-ray diffractometer of $Cu K\alpha$ radiation with a wavelength in the range of 1.54 \AA was used for XRD measurements. The radiations were incident on powder sample at the room temperature and diffracted angles of 2θ were recorded in the range of 20° to 60° . The XRD was made to operate at 40 kV and 30 mA. Then diffracted X-Rays intensities were recorded by using a scintillation detector.

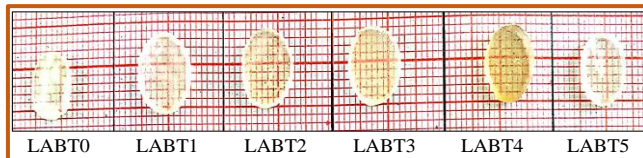


Figure 1. Images of prepared $(70-y) B_2O_3-20TeO_2-5Na_2O-5PbO-y(Eu_2O_3)$ glasses.

2.3 MAS-NMR measurements

The structural analysis of the formed glasses with and without europium trioxide was done using a high-resolution solid-state Bruker AV400 MAS-NMR spectrometer. The measurements were carried out successfully at room temperature. With a field strength of 9.39 Tesla and a frequency of 128.26 MHz, the equipment captured 11B MAS-NMR data. Also used for the measurements was a 90° pulse with a 2-second duration and a 2-second pulse delay.

2.4 Physical properties

The significant physical properties of glasses such as "density, molar volume, average boron-boron separation, interionic distance, polaron radius, rare-earth ion concentration, oxygen packing density (OPD), and field strength" were found by using the right mathematical relations [13-21]. The average boron-boron separation is one of the significant physical properties and was determined by using the formula:

$$\langle d_{B-B} \rangle = \left(\frac{V_m}{N_A \times X_B} \right)^{\frac{1}{3}} \quad (1)$$

Here, molar volume is denoted as V_m and X_B refers to the molar fraction of B_2O_3 in each glass sample and N_A is Avogadro's number. The mathematical equations were used to calculate the polaron radius and field strength of Eu^{3+} ions. [4,15-22]:

$$r_p = \frac{1}{2} \left(\frac{\pi}{6N_i} \right)^{\frac{1}{3}} \quad (2)$$

$$F = \frac{Z}{r_p^2} \quad (3)$$

N_i is the concentration of rare-earth ions, Z is the valency of the rare-earth ion, and r_p is the polaron radius. Equation (4) is used to calculate the oxygen packing density of glasses [19-22].

$$OPD = \frac{1000 \times O_n}{V_m} \quad (4)$$

Here, O_n is taken as the number of oxygen atoms in the glass samples.

2.5 UV-Visible spectrometer investigation

The obtained LABT glass samples were taken in the dimensions of thickness of 1.4 mm to 2 mm, and diameter of 0.8 cm to 1.2 cm.

To achieve parallel, shiny, and flat planes, the specimens were polished with adequate (P1500 grade) emery polishing paper. The Perkin-Elmer Lambda-30 absorption spectrophotometer was intended to work in the wavelength range of 200 nm to 1100 nm at room temperature.

2.6 Optical properties

With appropriate formulae, optical properties such as “dielectric constant, Urbach energy and steepness parameter, molar refraction, molar polarizability, reflection loss, metallic or non-metallic nature, electronic oxide polarizability, optical basicity, electronic negativity, and electronic susceptibility” have been determined [4,22-32].

3. Results and discussions

3.1 X-Ray Diffraction Analysis

Figure 2 depicts the spectra of the X-Ray diffraction pattern of ready LABT glasses. It is noticed from the diffraction patterns that, the presence of wide range scattering about small-angle sections in its place of crystalline peaks is essentially characteristic property of non-crystalline materials. Therefore, it can be stated that the prepared glasses exhibit a non-crystalline nature and short range atomic arrangement [1,11,14].

3.2 ¹¹B MAS-NMR Spectroscopy analysis

On ready glasses, ¹¹B MAS-NMR spectroscopy was used to evaluate structural expansion in the BO₃ and BO₄ units, which could occur during the production of LABT glasses. Figure 3 displays the ¹¹B MAS-NMR spectra of LABT glasses containing different amounts of europium, which shows two significant resonance peaks, one at 0.64 ppm and the other near 10 ppm to 13 ppm. The first peak, which is more intense and acute, is connected to the four coordinated BO₄ units in the glass system and is caused by a strong quadrupolar interaction. The second peak, which is somewhat broader and less intense than the first peak and is positioned between 10 ppm and 13 ppm, is categorized as a minor significant quadrupolar broadening and assigned to three coordinated BO₃ units [33-37].

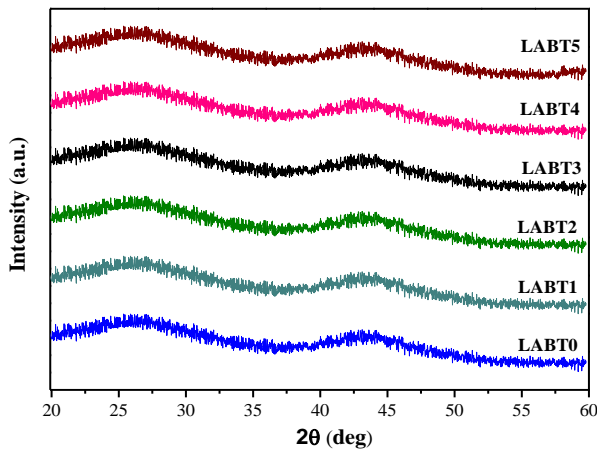


Figure 2. XRD pattern of (70-y) B₂O₃-15TeO₂-10Na₂O-5PbO-y(Eu₂O₃) glasses.

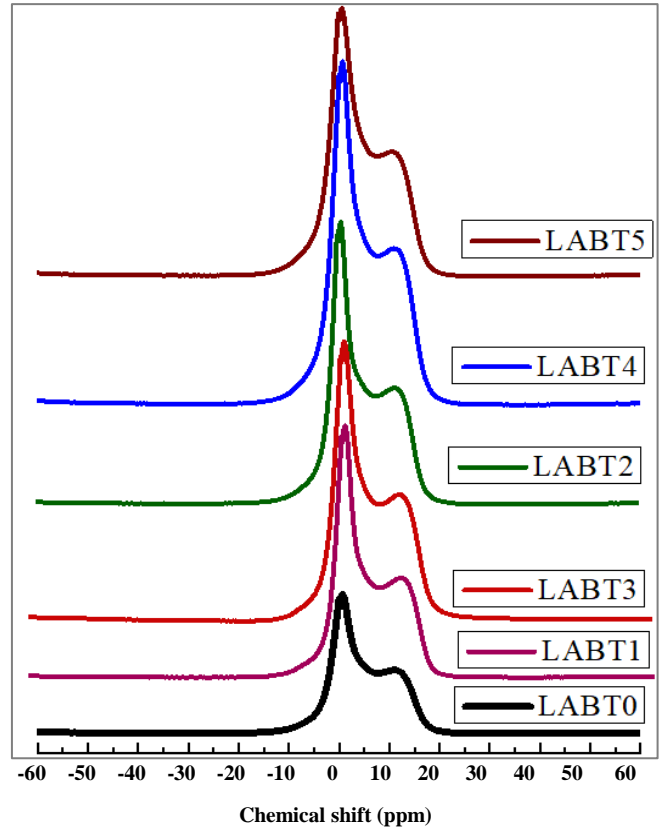


Figure 3. ¹¹B MAS-NMR spectra of LABT glasses.

3.3 Physical properties

The density and molar volume of LABT glasses were estimated by Archimedes' principal [1] and are shown in Figure 4. The average d_{B-B} distance is determined to test the impact of Eu₂O₃ on the variation of glass structure and obtained d_{B-B} values vary with change in Eu₂O₃ concentration. The d_{B-B} values of LABT glasses range from 4.846 to 5.254 Å. In Figure 4, not only the reverse nature of density and molar volume was noticed, but the modification of densities and molar volume due to the addition of europium trioxide was also observed. The significant variations in the density are attributed to i) larger changes in average molecular weight in oxide ions of glass owing to the higher molecular weight of Eu₂O₃ than B₂O₃, ii) considerable changes in molar mass of europium trioxide, iii) addition of lead ions with Eu³⁺ ions holds greater atomic mass. Additionally, the generation of non-bridging oxygen (NBO) in LABT glasses also impacts modifications in density, and similar work is also reported in the literature [1,9,11,20, 38-41]. It is noticed that the density of glasses has been increased up to LABT2 glasses with rise in concentration of Eu₂O₃ and decreased at LABT3 and LABT4 glasses. The density is increased yet again for LABT5 glass. The highest density is reported for the 0.2 mol% (LABT2) glass as 3.205 g·cm⁻³ which is due to significant changes occurred in glass network which leads to the less generation of non-bridging oxygens. In Figure 5 it is noticed that both polaron radius and interionic distance are decreased with increasing of Eu³⁺ ions as reported in Table 1. Because of contracted and distorted lattice sites, and a decrease in the interionic distance, the polaron radius decreased with an increase in Eu³⁺ ion concentration in ready glasses.

Table 1. Density(ρ), molar volume(V_m), Boron-Boron separation (d_{B-B}), rare earth ion concentration (N_i), Polaron radius (r_p), Inter ionic distance (R_i), Field strength (F), and Oxygen packing density (OPD).

Sample	y mol%	ρ ($\text{g}\cdot\text{cm}^{-3}$)	V_m (cm^3)	d_{B-B} (nm)	N_i ($\text{ions}\cdot\text{cm}^{-3}$)	r_p (\AA)	R_i (\AA)	F ($10^{14}\times\text{cm}^{-2}$)	OPD ($\text{g}\cdot\text{atom}\cdot\text{L}^{-1}$)
		± 0.001	± 0.001	± 0.001	± 0.001	± 0.001	± 0.001	± 0.001	± 0.001
LABT0	0	2.523	52.424	5.254	-	-	-	-	46.162
LABT1	0.1	2.957	44.803	4.980	4.033	11.749	3.072	2.173	54.014
LABT2	0.2	3.205	41.406	4.846	8.728	9.083	2.254	3.635	58.445
LABT3	0.3	2.828	47.001	5.049	11.533	8.277	2.054	4.378	51.489
LABT4	0.4	2.717	49.019	5.104	14.746	7.626	1.892	5.157	49.374
LABT5	0.5	2.935	45.441	4.982	19.881	6.903	1.713	6.294	53.255

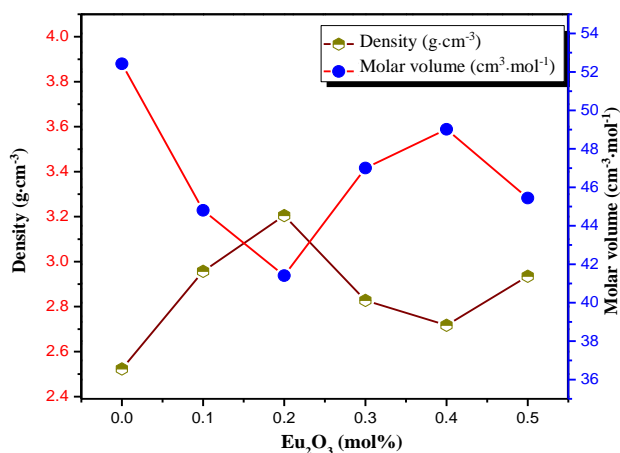


Figure 4. Density and molar volume variation against mol% of Eu_2O_3

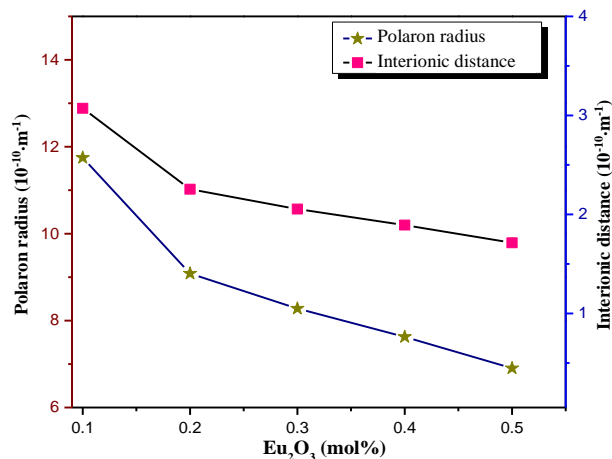


Figure 5. Polaron radius and Interionic distance variations with mol% of Eu_2O_3 .

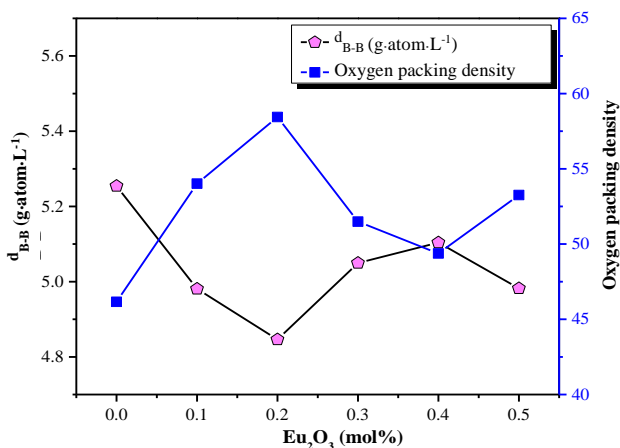


Figure 6. Average boron-boron separation and OPD changes versus mol% of Eu_2O_3

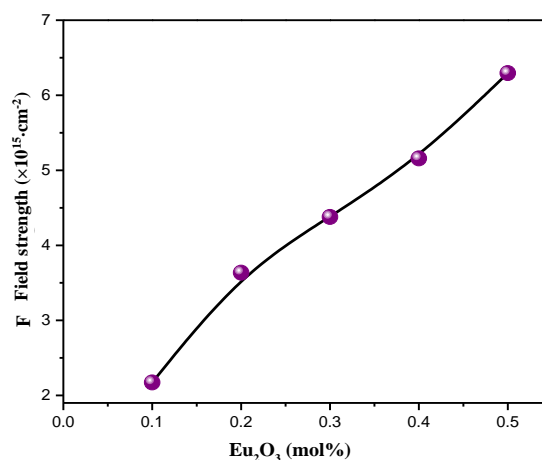


Figure 7. Plot of field strength versus mol% of Eu_2O_3

The oxygen packing density (OPD) provides the idea of an array of oxygen atoms in oxide glass. In Figure 6, the average boron-boron separation and OPD variations with Eu_2O_3 concentration are depicted. The improvement in Eu_2O_3 doping accompanies the variations of molar volume and it also signifies the hardness of oxide glass. The improvement in NBO atoms and extension of the structure is described by the changes in OPD with Eu_2O_3 content [1,11,41-43]. Figure 7 depicts the relationship between field strength and Eu_2O_3 concentration. The attractive interactions between ions and nearby structural units grow as the concentration of Eu^{3+} ions rises. As a result, field strengths increase as the interionic distance decreases [4,44].

3.4 Optical properties

The absorption spectra of all LABT glasses and LABT5 shown in Figure 8. The plot of LABT5 consists of seven prominent and sharp peaks situated at 394, 417, 466, 525, 534, 578, and 587 nm which are due to the electronic transitions of ${}^7\text{F}_0\text{-}{}^5\text{L}_6$, ${}^7\text{F}_1\text{-}{}^5\text{D}_3$, ${}^7\text{F}_0\text{-}{}^5\text{D}_2$, ${}^7\text{F}_0\text{-}{}^5\text{D}_1$, ${}^7\text{F}_1\text{-}{}^5\text{D}_1$, ${}^7\text{F}_0\text{-}{}^5\text{D}_0$ and ${}^7\text{F}_1\text{-}{}^5\text{D}_0$, respectively. For all glass samples, the absorption coefficient i.e. $\alpha(\nu)$ was measured near the absorption edge at photon energies. It has been reported that direct and indirect bandgap data well fit an Equation (5) proposed by Davis and Mott. [1,9,18,20,21,40-46].

$$\alpha(h\nu) = \left(\frac{B}{h\nu}\right) (h\nu - E_{opt})^m \quad (5)$$

$$\alpha(\lambda) = 2.303 \left[\frac{A}{d}\right] \quad (6)$$

Here, A is the absorbance, d is the thickness of the LABT glass samples, and m indicates an index that has values such as 2, 1/2, 3/2,

and 3 corresponding to indirect allowed, direct allowed, direct forbidden, and indirect forbidden respectively, B is a constant which indicates the band tailing parameter, $h\nu$ is photon energy and E_{opt} is the optical energy bandgap. The direct and indirect bandgap energy values were found by Tauc's plots and those plots are denoted in Figure 9.

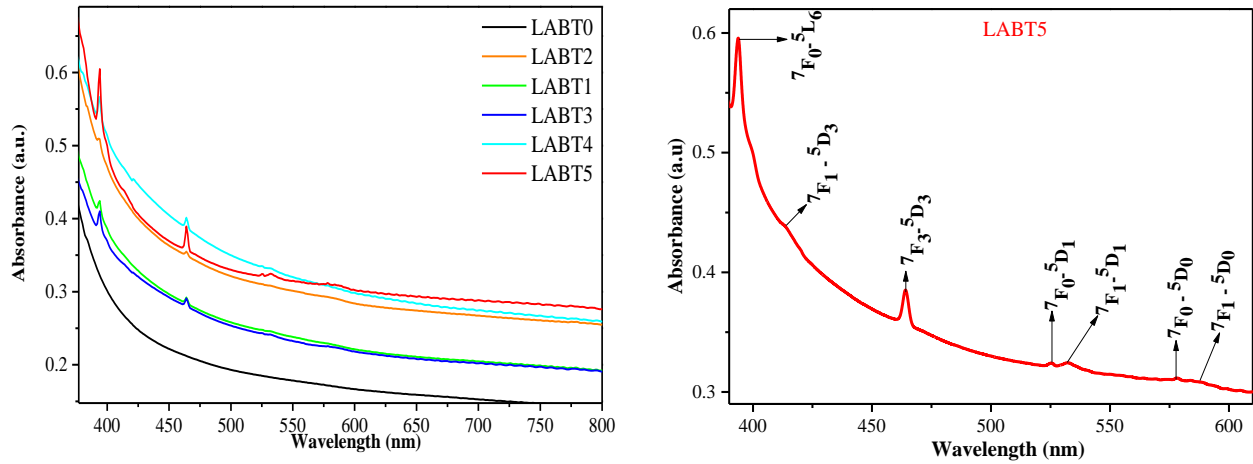


Figure 8. Optical absorption spectra of the LABT Glasses and LABT5 glass.

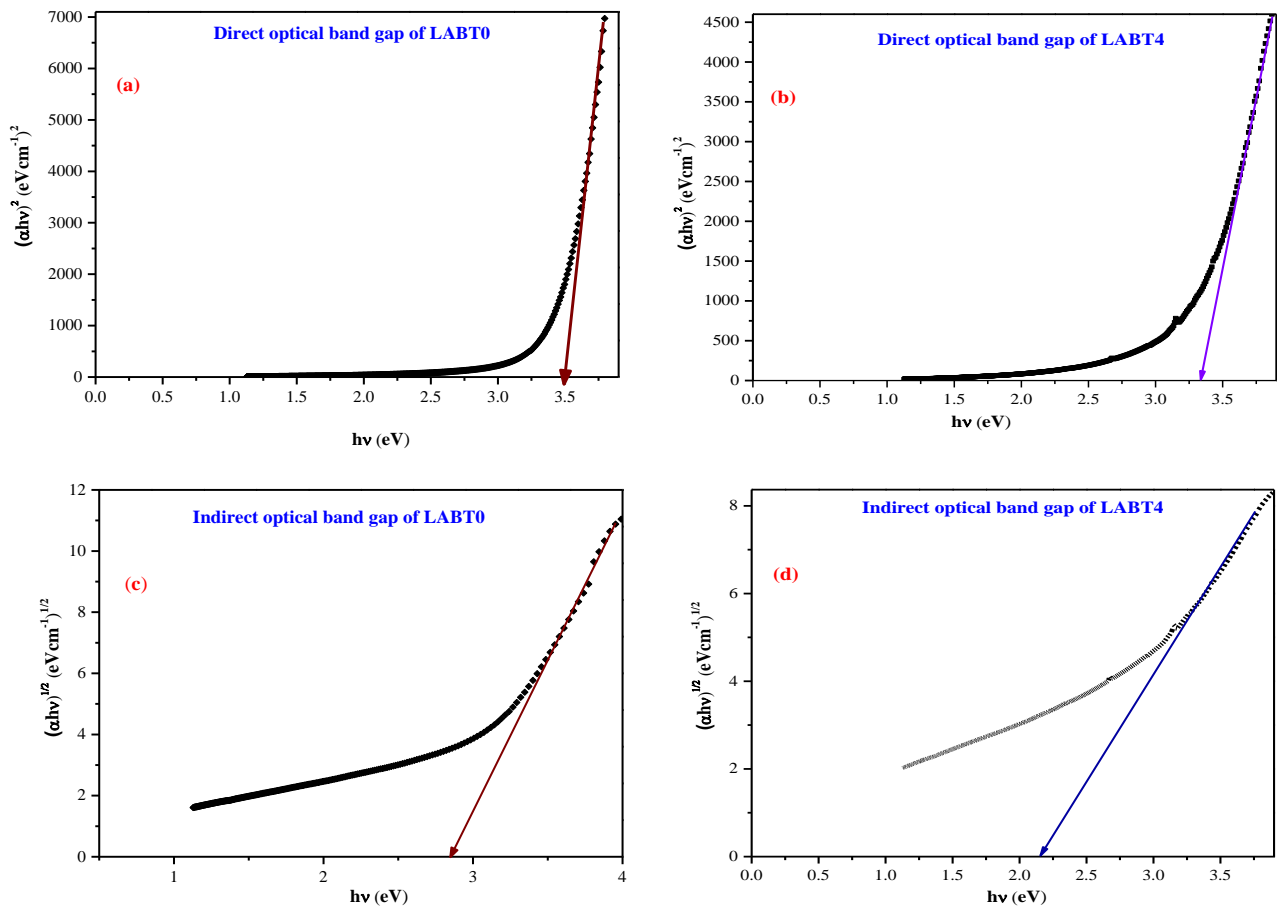


Figure 9. (a) and (b) Typical plot of Variation of $(ah\nu)^2$ versus $h\nu$ of LABT0 and LABT4 glasses, (c) and (d) Typical plot of Variation of $(ah\nu)^{1/2}$ versus $h\nu$ of LABT0 and LABT4 glasses.

The variation in the bandgap energy of boro tellurite glasses with increasing Eu_2O_3 concentration has been ascribed to the formation of Eu_2O_3 clusters in the glass matrix, which create defect states in the bandgap of the glass. These defect states act as traps for charge carriers, leading to a significant modifications in the bandgap energy. The optical direct energy bandgap values for LABT glasses are increased up to 0.3 mol% and decreased at 0.4 mol% and then after the E_g is yet again increased for 0.5 mol%, the same kind of observations are also reported [8,31]. The optical direct energy bandgap and indirect energy bandgap are depicted in Figure 10. Obtained direct and indirect bandgap values lay between 3.367 to 3.653 eV and 2.019 to 3.021 eV, respectively. The significant variations in the bandgap values with the addition of Eu^{3+} ions into the glass were noticed which is mainly because of the formation of NBOs. The addition of Eu_2O_3 results in the glasses' new structural alterations and a larger number of NBOs, which modifies the value of bandgap. The increase in Eu^{3+} concentration is consequently attributed to an increase in bandgap energies, which may demagnify the degree of localization by causing a defect in the charge distribution and pushing the nearest oxygen ions' energy levels closer to the top of the valence band, raising donor centers in the glass matrix. The energy band gap narrows because of the rise of donor centers.

Urbach energy is the parameter that measures the disorders in both crystalline and noncrystalline materials. It can be measured by relation (7) and by taking the reciprocal of the slope at the linear region of curves in the plot of $\ln(\alpha)$ versus $h\nu$ and as shown in Figure 11.

$$\ln\alpha = \ln\alpha_o + \frac{h\nu}{\Delta E} \quad (7)$$

The obtained results affirm considerable variations originated from the addition of Eu_2O_3 into the glass network. The highest disorderliness was obtained for the LABT2 glass. The variations in Urbach energy are ascribed to the transformation from weak bonds to defects, this leads to improvement in the disorder in the glass structure. The variations of Urbach energy and steepness parameter versus rare earth concentration are shown in Figure 12. These disorders have a greater influence on more restricted states when band gaps exist. It has been observed that ΔE values can be used to determine the structural stability of glasses [4,41,45]. The lower the ΔE values, the more stable the glass structure will be. With the addition of Eu_2O_3 , it is observed that the ΔE values change, indicating changes in structural strength, as well as alterations in the degree of the defect and electron delocalization. The steepness parameter can be used to investigate the relaxation of exciton-phonon or electron-phonon due to

the expansion of optical absorption (S). The obtained values of the steepness parameter of LABT glasses are in the range of 0.0416 to 0.0556, which accomplishes the less temperature dependence.

An important and more useful parameter i.e., refractive index was evaluated by a Lorentz- Lorentz equation (8), here E_g refers to the energy gap.

$$\frac{n^2-1}{n^2-2} = 1 - \frac{\sqrt{E_g}}{20} \quad (8)$$

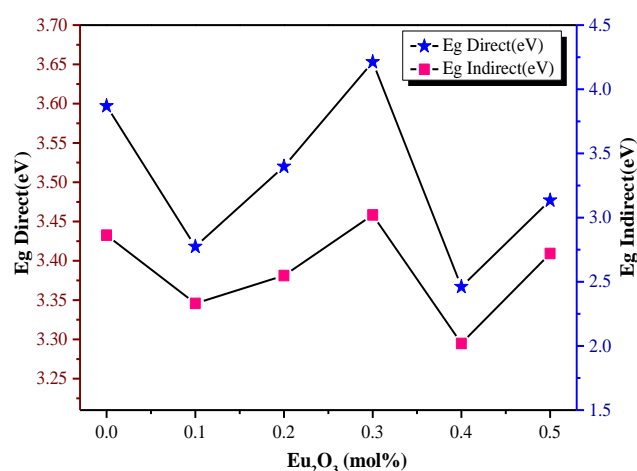


Figure 10. Optical direct energy gap and indirect energy variations with Eu_2O_3 mol%.

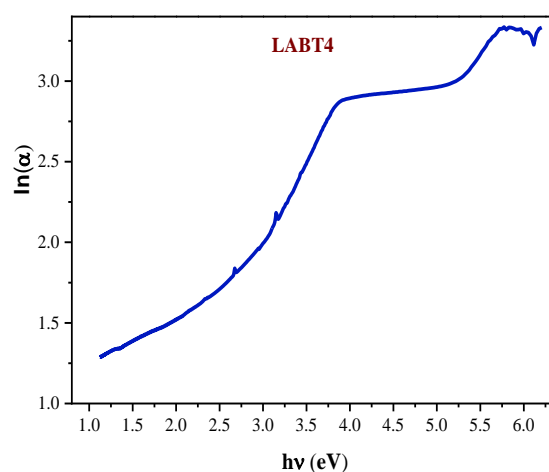


Figure 11. $\ln(\alpha)$ versus $h\nu$ for LABT4 glass.

Table 2. Eu_2O_3 (mol%), Optical direct band gap $E_{g(d)}$ (eV), optical indirect band gap $E_{g(ind)}$ (eV), Urbach energy ΔE (eV), Steepness Parameter (S), Molar refraction (R_m), Optical dielectric constant (K), Reflection loss- R_L (%), Electronic molar polarizability- α_m (\AA^3), Metallization criterion (M).

y mol%	$E_{g(d)}$	$E_{g(ind)}$	ΔE	S	R_m	K	R_L	α_m	n	M
	± 0.001	± 0.001	± 0.01	± 0.001	± 0.001	± 0.001	± 0.001	± 0.001	± 0.01	± 0.001
0	3.510	2.863	0.46	0.055	35.257	5.107	0.672	1.399	2.26	0.327
0.1	3.418	2.331	0.59	0.043	31.143	5.560	0.695	1.235	2.35	0.304
0.2	3.520	2.548	0.62	0.041	27.925	5.143	0.674	1.108	2.26	0.325
0.3	3.653	3.021	0.60	0.043	31.391	5.022	0.667	1.245	2.24	0.332
0.4	3.375	2.019	0.56	0.045	33.434	5.294	0.682	1.326	2.30	0.317
0.5	3.477	2.72	0.47	0.054	30.768	5.193	0.677	1.220	2.27	0.323

Further, with the knowledge of the refractive index, the dielectric constant, molar refraction, molar polarizability, reflection loss, and metallization criterion were determined with precise mathematical formulae [16,20-24]. The obtained values are tabulated in Table 2. The optical refractive index and dielectric constant vary nonlinearly with the addition of Eu₂O₃ content as shown in Figure 13. This is due to perturbation in the glass structure with the insertion of europium trioxide, which leads to a disturbance inside the glass network by increasing NBO atoms. The highest refractive index is reported for LABT1 glass. Further, the significant modifications in the refractive index are owing to considerable improvement in NBO atoms.

The important parameter reflection loss (R_L) is calculated by the ratio of molar refraction to the molar volume. It is seen that the obtained R_L values vary with the addition of Eu₂O₃ mol%. The indication of the non-metallic and metallic nature of solids can be engaged by using the metallization criterion [46-49]. Additionally, Dimitrov and Komatsu [25,28,29,50] recommended the metallization criterion for most of the oxide glasses by using the Lorentz-Lorentz relation, with optical bandgap and static refractive index. The values of R_L are useful to find the metallization criterion values.

The perceptions proposed by Xinyu Zhao *et al.*, [51] give the idea about the non-metallic nature of solids which is based on the metallization criterion. The reflection loss R_L greater than or equal to one indicates the metallic nature of solids and R_L values less than one shows the nonmetallic nature of solids [52]. The obtained R_L values of LABT glasses range from 0.6678 to 0.6951 and the metallization criterion values vary from 0.304 to 0.332. Additionally, the values are matching with non-linear optical values 0.3 to 0.4 [26,50-52]. The addition of Eu₂O₃ into the glass network influences the metallization criterion values. In this kind of development, the influence of increase in both the valence and conduction bands arises with narrowing the bandgap. As a result, the produced glasses have a nonmetallic appearance. As a result, the established values of LABT glasses make them appropriate for optical computing, optical data storage, and optical switching applications [49,53].

3.5 Electronic negativity, Electron oxide polarizability, Optical basicity, Electronic susceptibility

The very important factors of LABT glasses such as electronic negativity (χ), electron polarizability (α_0), optical basicity (\wedge) and electric susceptibility (χ_e) [24-30] were estimated by mathematical equations; and obtained values are tabulated in Table 3.

$$\chi = 0.2688E_g \quad (9)$$

$$\alpha_0 = 0.9\chi + 3.5 \quad (10)$$

$$\wedge = 0.5\chi + 1.7 \quad (11)$$

$$\chi_e = \frac{n^2-1}{4\pi} \quad (12)$$

In equations, E_g denotes the optical direct energy bandgap, and n refers to the refractive index.

“Dimitrov, Sakka, and Komatsu” proposed appreciated relations for electronegativity, optical basicity, and cation polarizability of oxide ions [29,54,55]. The term "electronegativity" refers to the strength with which an ion can attract electrons, this also holds good for all oxide glasses.

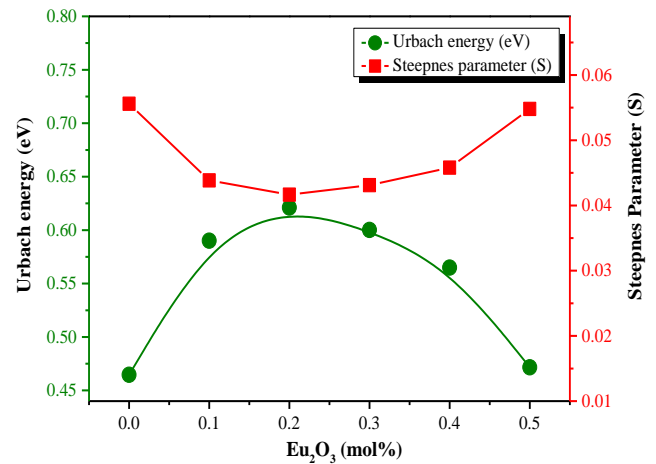


Figure 12. Variation of Urbach energy and steepness parameter versus Eu₂O₃ mol%.

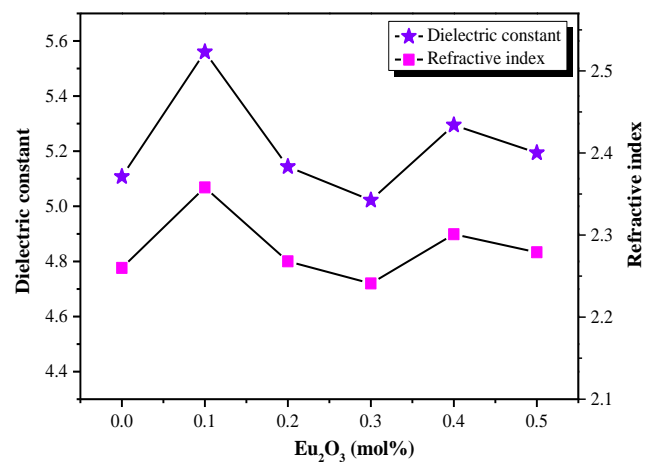


Figure 13. Variation of refractive index and dielectric constant versus Eu₂O₃ mol%.

Table 3. Electronic negativity (χ), electron polarizability (α_0), optical basicity (\wedge), and electric susceptibility (χ_e).

Sample	y mol%	χ ±0.001	α_0 ±0.001	\wedge ±0.0001	χ_e ±0.001
LABT0	0	0.966	2.630	1.217	0.3268
LABT1	0.1	0.918	2.673	1.241	0.3628
LABT2	0.2	0.946	2.648	1.227	0.3297
LABT3	0.3	0.982	2.616	1.209	0.3200
LABT4	0.4	0.905	2.685	1.247	0.3417

The greater the value of electronegativity, the more powerful the pull of ions towards the bonded oxide ions. This causes the tight bonding between ions in the glass structure, which in turn leads to the development of covalent nature in the material. As predictable, it is observed that χ values that were calculated with optical direct energy bandgap are changing with an increase in molar concentration of Eu_2O_3 and the highest χ value reported for LABT3 glass is 0.982. Figure 14 depicts the variation of electronic negativity and electric susceptibility with a molar concentration of Eu_2O_3 and Figure 15 portrays the variation of optical basicity versus molar concentration of Eu_2O_3 .

The ability of the glasses to deliver a negative charge to the glass ion is referred to as optical basicity [28,29,49,51]. The LABT glasses' optical basicity was investigated, and the results show that these glasses can give negative charges to neighboring cations. The oxygen-cation bonds become more covalent because of this [53]. Modifications in optical basicity with an increased rare-earth ion concentration in glasses were used to investigate improvements in ionic chemical bond to covalent chemical bond conversions. Because a rise in optical basicity weakens the metal-oxide link, the covalent character of the bond may be reduced. This type of ionic behavior accepts the formation of non-bridging oxygen atoms (NBOs) in the investigated LABT glasses.

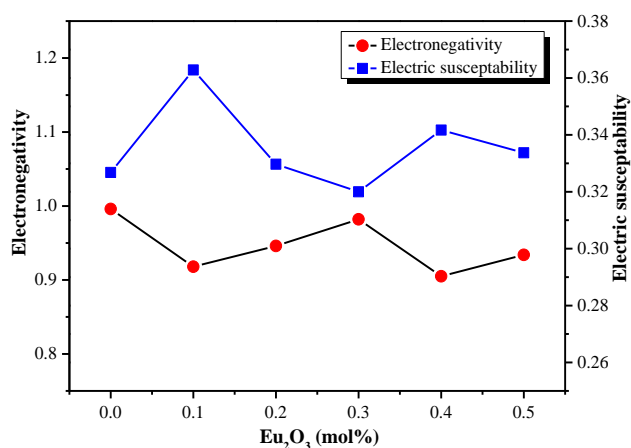


Figure 14. Plot of electronic negativity and electric susceptibility with Eu_2O_3 mol%.

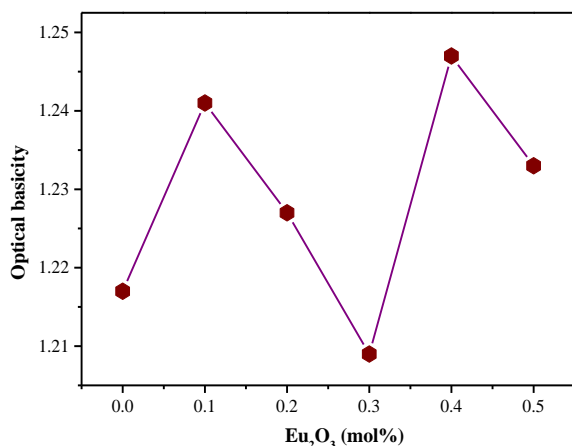


Figure 15. Plot of optical basicity versus Eu_2O_3 mol%.

Additionally, it is also proved by experimentally calculated dropping of energy bandgaps [25,55]. The obtained results of physical and optical properties and other significant structural parameters suggest that the investigated glasses are potential candidates for europium-doped fiber amplifier applications and possible optical switching applications, optical computing, optical data storage, and broadband appliances [1,15,17,20,39,40,45].

4. Conclusion

The conventional melt quenching method was used to produce the europium trioxide dope alkali Lead Boro-Tellurite Glasses. The non-crystalline structure was affirmed by XRD patterns. The considerable changes in density, molar volume, and other physical properties were analyzed and this is due to the generation of non-bridging oxygen and modifications in OPD. The structural changes and structural stability of glasses were deliberated with ^{11}B MAS-NMR spectroscopy. It confirms the occurrence of quadrupolar broadening in BO_3 units and quadrupolar interactions in BO_4 in all LABT glasses. The addition of Eu_2O_3 gives important modifications to NBOs within LABT glasses. The optical energy band gap was found to be having variations with raising the concentration of Eu_2O_3 which is due to shifting of the absorption edge. Optical properties were found to be undergoing significant variations by increasing Eu_2O_3 concentration. The highest refractive index is found at 2.358 for glass LABT2 and the lowest one is found at 2.241 for LABT3 glass which is because of NBOs. Significant alterations in the metallization criterion are described, as well as signs of effective changes in optical bandgap energies and Urbach energy. The reported steepness parameter values support the hypothesis of less temperature dependence. Ionic nature and its considerable variations are shown by changes in parameters such as electronegativity and electronic polarizability for prepared glasses. Overall, the newly prepared glasses with their "structural stability, refractive index, metallization criterion, optical dielectric constant, electronegativity, and electronic polarizability" suggest potential applications in developing fibre manufacture, optical switching.

Acknowledgements

The authors would like to thank i). Manipal Institute of Technology Bengaluru, MAHE Manipal for extensive encourage and support for research, ii). IISc, Bengaluru for providing equipment's for spectroscopy characterizations, iii) V. Dimitrov, S. Sakka, and T. Komatsu for the procedures that contributed to the measure of electronic polarizability, non-linear optical properties, and optical basicity of oxide glasses.

References

- [1] C. Devaraja, G. V. Jagadeesha Gowda, B. Eraiah, "Physical, structural and photoluminescence properties of lead boro-tellurite glasses doped with Eu^{3+} ions," *Vacuum*, vol. 177, p. 109426, 2020.

- [2] T. Hasegawa, "Optical properties of Bi₂O₃-TeO₂-B₂O₃ glasses," *Journal of non-crystalline solids*, vol. 357, pp. 2857-2862, 2011.
- [3] M. Reza Dousti, Raja J. Amjad, "Effect of silver nanoparticles on the upconversion and near-infrared emissions of Er³⁺:Yb³⁺ co-doped zinc tellurite glasses," *Measurement*, vol. 105, pp. 114-119, 2017.
- [4] C. Devaraja, G. V. Jagadeesha Gowda, B. Eraiah, "Optical properties of bismuth tellurite glasses doped with holmium oxide," *Ceramics International*, vol. 47, pp. 7602-7607, 2021.
- [5] N. Deopa, A.S. Rao, "Spectroscopic studies of single near ultraviolet pumped Tb³⁺ doped lithium lead alumino borate glasses for green lasers and tri-colour w-LEDs," *Journal of luminescence*, vol. 194, pp. 56-63, 2018.
- [6] N. Sooraj Hussain, G. Hungerford, R. El-Mallawany, M. J. M. Gomes, M. A. Lopes, Nasar Ali, J. D. Santos, S. Buddhudu, "Absorption and emission analysis of RE³⁺ (Sm³⁺ and Dy³⁺): lithium boro tellurite glasses", *Journal of Nanoscience and Nanotechnology*, vol. 9, pp. 3 672-3678, 2009.
- [7] C. Devaraja, G. V. Jagadeesha Gowda, and B. Eraiah, "FTIR and Raman studies of Eu³⁺ ions doped alkali boro tellurite glasses," *AIP Conference Proceedings*, vol. 2115, pp. 1-5, 2019.
- [8] El-Mallawany, R. A. "Optical properties of boro-tellurite glasses containing europium oxide", *Journal of Non-Crystalline Solids*, vol. 357, pp. 714-719, 2011.
- [9] C. Devaraja, and G. V. Jagadeesha Gowda, "DC conductivity of heavy metal oxide (Bi₂O₃) boro-tellurite glasses: Effect of Eu₂O, *Journal of Metals, Materials and Minerals*, vol. 32, no. 2, pp. 77-82, 2022.
- [10] R. Rajaramakrishna, C. Wongdeeying, P. Yasaka, P. Limkitjaroenporn, N. Sangwanate, and J. Kaewkhao, "Pr³⁺ doped BaO:ZnO: B₂O₃:TeO₂ glasses for laser host matrix," *Journal of Metals, Materials and Minerals*, vol. 28, no. 2, pp. 47-54, 2019.
- [11] C. Devaraja, G. V. Jagadeesha Gowda, and B. Eraiah, "Structural, thermal and spectroscopic studies of europium trioxide doped lead boro-tellurite glasses," *Journal of alloys and compounds*, vol. 871, p. 159585, 2021.
- [12] R. Cao, Y. Lu, Y. Tian, F. Huang, S. Xu, and J. Zhang, "Spectroscopy of thulium and holmium co-doped silicate glasses," *Optical Material Express*, vol. 6, p. 2252, 2016.
- [13] R. S. Kundu, S. Dhankhar, R. Punia, K. Nanda, and N. Kishore, "Bismuth modified physical, structural and optical properties of mid-IR transparent zinc boro-tellurite glasses," *Journal of Alloys and Compounds*, vol. 587, pp. 66-73, 2014.
- [14] C. Devaraja, G. V. Jagadeesha Gowda, and B. Eraiah, "Structural, conductivity, and dielectric properties of europium trioxide doped lead boro-tellurite glasses," *Journal of Alloys and Compounds*, vol. 898, p. 162967, 2022.
- [15] C. Devaraja, G. V. J. Gowda, B. Eraiah, and G. K N. Murthy, "Elastic properties of boro-tellurite glasses doped with europium oxide," *Journal of Metals, Materials and Minerals*, vol. 32, no. 2, pp. 56-62, 2022.
- [16] B. Srinivas, A. Hameed, M.N. Chary, and Md Shareefuddin, "Physical, optical and FT-IR studies of bismuth-boro-tellurite glasses containing BaO as modifier," *IOP Conference Series, Material Science and Engineering*, vol. 360, p. 012022, 2018.
- [17] K. Swapna, S. Mahamuda, A. S. Rao, T. Sasikala, P. Packiyaraj, L. R. Moorthy, and G. V. Prakash, "Luminescence characterization of Eu³⁺ doped zinc alumino bismuth borate glasses for visible red emission applications," *Journal of Luminescence*, vol. 156, pp. 80-86, 2014.
- [18] G. V. Jagadeesha Gowda, and B. Eraiah, "Optical properties of praseodymium doped silver-borate glasses," *Canadian Journal of Physics*, vol. 1157, pp. 1154-1157, 2014.
- [19] A. A. Ali, H. M. Shaaban, and A. Abdallah, "Spectroscopic studies of ZnO borate-tellurite glass doped with Eu₂O₃", *Journal of Materials Research and Technology*, vol. 7, pp. 240-247, 2018.
- [20] M. Shwetha, and B. Eraiah, "Influence of europium (Eu³⁺) ions on the optical properties of lithium zinc phosphate glasses," *IOP Conference Series, Material Science and Engineering*, vol. 310, p. 012033, 2018.
- [21] A. Usman, M. K. Halimah, A. A. Latif, F. D. Muhammad, and A. I. Abubakar, "Influence of Ho³⁺ ions on structural and optical properties of zinc borotellurite glass system," *Journal of Non Crystalline Solids*, vol. 483, pp. 18-25, 2018.
- [22] M. N. Azlan, M. K. Halimah, S. Z. Shafinas, and W. M. Daud, "Polarizability and optical basicity of Er³⁺ ions doped tellurite based glasses," *Chalcogenide Letters*, vol. 11, pp. 319-335, 2014.
- [23] A. H. Hammad, H. M. Elsaghier, W. Abbas, N. A. Zidan, and S. Y. Marzouk, "Investigation of some structural and optical properties of lithium sodium fluoroborate glasses containing cuprous oxide," *Measurement*, vol. 116, pp. 170-177, 2018.
- [24] T. R. Tasheva, V. Dimitrov, "Electronic polarizability, optical basicity and chemical bonding of zinc oxide-barium oxide-vanadium oxide glasses," *Bulgarian Chemical Communications*, vol. 49, pp. 76-83, 2017.
- [25] V. Dimitrov, "Classification of simple oxides: A polarizability approach," *Journal of Solid State Chemistry*, vol. 163, pp. 100-112, 2002.
- [26] X. Zhao, X. Wang, H. Lin, and Z. Wang, "Electronic polarizability and optical basicity of lanthanide oxides," *Physica B: Condensed matter*, vol. 392, pp. 132-136, 2007.
- [27] X. Zhao, X. Wang, H. Lin, and Z. Wang, "Average electronegativity, electronic polarizability and optical basicity of lanthanide oxides for different coordination numbers," *Physica B: Condensed matter*, vol. 403, pp. 1787-1792, 2008.
- [28] V. Dimitrov, and T. Metallurgy, "Electronic polarizability, optical basicity and single bond strength of oxide glasses," *Journal of Chemical Technology and Metallurgy*, vol. 48, pp. 549-554, 2013.
- [29] V. Dimitrov, and T. Komatsu, "Electronic polarizability, optical basicity and non-linear optical properties of oxide glasses", *Journal of Non Crystalline Solids*, vol. 249, pp. 160-179, 1999.
- [30] R. K. Brow, and D. R. Tallant, "Structural design of sealing glasses," *Journal of Non Crystalline Solids*, vol. 222, pp. 396-406, 1997.

- [31] El-Mallawany, R. A. H. "Influence of europium oxide concentration on electrical switching properties of borotellurite glasses." *Journal of Materials Science*, vol. 48, pp. 2054-2063, 2013.
- [32] K. Vosejpkova, L. Koudelka, Z. Cernosek, P. Mosner, L. Montagne, and B. Revel, "Structural studies of boron and tellurium coordination in zinc borophosphate glasses by ^{11}B MAS NMR and raman spectroscopy," *Journal of Physics and Chemistry of Solids*, vol. 73, pp. 324-329, 2012.
- [33] G. Jellison, P. Bray, "A structural interpretation of ^{10}B and ^{11}B NMR spectra in sodium borate glasses", *Journal of Non Crystalline Solids*, vol. 29, pp. 187-206, 1978.
- [34] W. J. Dell, P. J. Bray, and S. Z. Xiao, " ^{11}B NMR studies and structural modelling of $\text{Na}_2\text{O}-\text{B}_2\text{O}_3-\text{SiO}_2$ glasses of high soda content," *Journal of Non Crystalline Solids*, vol. 58, pp. 1-16, 1983.
- [35] R. E. Youngman, and J. W. Zwanziger, "On the Formation of Tetracoordinate boron in rubidium borate glasses," *Journal of the American Chemical Society*, vol. 117, pp. 1397-402, 1995.
- [36] J. S. Wu, M. Potuzak, and J. F. Stebbins, "High-Temperature in situ ^{11}B NMR study of network dynamics in boron-containing glass-forming liquids," *Journal of Non Crystalline Solids*, vol. 357, pp. 3944-3951, 2011.
- [37] P. Venkata Kala, K. Srinivasarao, D. Krishna Rao, "Dielectric and spectroscopic properties of CuO doped LiF-PbO-B $_2$ O $_3$ glasses", *Physics and Chemistry of Glasses: European Journal of Glass Science and Technology Part B*, vol. 57, pp. 166-172, 2016.
- [38] P. Rehana, O. Ravi, B. Ramesh, G.R. Dillip, and C.M. Reddy, "Photoluminescence studies of Eu $^{3+}$ ions doped calcium zinc niobium borotellurite glasses," *Advanced Material Letters*, vol. 7, pp. 170-174, 2016.
- [39] P. Aryal, C. R. Kesavulu, H. J. Kim, S. W. Lee, S. J. Kang, J. Kaewkhao, N. Chanthima, B. Damdee, "Optical and luminescence characteristics of Eu $^{3+}$ - doped B $_2$ O $_3$:SiO $_2$:Y $_2$ O $_3$:CaO glasses for visible red laser and scintillation material applications", *Journal of Rare Earths*, vol. 36, pp. 482-491, 2017.
- [40] K. Maheshvaran, and K. Marimuthu, "Optical studies on Eu $^{3+}$ doped boro-tellurite glasses," *AIP Conference Proceedings*, vol. 1447, p. 549, 2012.
- [41] N. B. Shigihalli, R. Rajaramkrishna, and R. V Anavekar, "Optical and radiative properties of Nd $^{3+}$ - doped lead tellurite borate glasses", *Canadian Journal of Physics*, vol.6, pp. 322-327, 2013.
- [42] I. Zaitizila, M. K. Halimah, F. D. Muhammad, and M. S. Nurisya, "Thermal stability, structural and optical properties of Rice husk silica borotellurite glasses containing MnO $_2$ ", *Chalcogenide Letters*. vol. 15, pp. 187-197, 2018.
- [43] A. Kaur, A. Khanna, C. Pesquera, and B. Chen, "Structural, optical, dielectric and thermal properties of molybdenum tellurite and borotellurite glasses," *Journal of Non Crystalline Solids*, vol. 444, pp. 1-10, 2016.
- [44] L. Singh, V. Thakur, R. Punia, R.S. Kundu, and A. Singh, "Structural and optical properties of barium titanate modified bismuth borate glasses," *Solid State Science*, vol. 37, pp. 64-71, 2014.
- [45] F. Zaman, "Physical, structural and luminescence investigation of Eu $^{3+}$ -doped lithium- gadolinium bismuth-borate glasses for LEDs," *Solid State Science*, vol. 80, pp. 161-169, 2018.
- [46] S. Selvi, K. Marimuthu, N. Suriya Murthy, and G. Muralidharan, "Red light generation through the lead boro-telluro-phosphate glasses activated by Eu $^{3+}$ ions", *Journal of Molecular Structure*. vol. 1119, pp. 276-285, 2016.
- [47] B. Bhatia, S.L. Meena, V. Parihar, and M. Poonia, "Optical basicity and polarizability of Nd $^{3+}$ - Doped bismuth borate glasses," *New Journal of Glass and Ceramics*, vol. 5, pp. 44-52, 2015.
- [48] Adel. I. Kashif, and A. Ratep, "Polarizability, optical basicity and optical properties of SiO $_2$ B $_2$ O $_3$ Bi $_2$ O $_3$ TeO $_2$ glass system", *Applied Physics A*, vol. 124, p. 486, 2018.
- [49] V. Thakur, A. Singh, R. Punia, M. Kaur, and L. Singh, "Effect of BaTiO $_3$ on the structural and optical properties of lithium borate Effect of BaTiO $_3$ on the structural and optical properties of lithium borate glasses," *Ceramic International*, vol. 41, pp. 10957-10965, 2015.
- [50] V. Dimitrov, and T. Komatsu, "An interpretation of optical properties of oxides and oxide glasses in terms of the electronic ion polarizability and average single bond strength, *Journal of the University of Chemical Technology and Metallurgy*, vol. 45, pp. 219-250, 2010.
- [51] X. Zhao, X. Wang, H. Lin, and Z. Wang, "Average electronegativity, electronic polarizability and optical basicity of lanthanide oxides for different coordination numbers," *Physica B: Condensed Matter*, vol. 403, pp. 1787-1792, 2008.
- [52] D. B. Thombre, "The Estimation of oxide polarizability and basicity using electronegativity for B $_2$ O $_3$: M $_2$ O glass system (M = Li, Na, K, Rb)," *International Journal of Innovative Science, Engineering & Technology*, vol. 3, pp. 449-453, 2016.
- [53] M. K. Halimah, M. F. Faznny, M. N. Azlan, and H. A. A Sidek, "Optical basicity and electronic polarizability of zinc borotellurite glass doped La $^{3+}$ ions, *Results in Physics*, vol. 7, pp. 581-589, 2017.
- [54] V. Dimitrov, S. Sakka, and V. Dimitrov, "Linear and nonlinear optical properties of simple oxides," *Journal of Applied Physics*, vol. 79, pp. 1741-1745, 1996.
- [55] V. Dimitrov, and T. Komatsu, "Classification of oxide glasses : A polarizability approach," *Journal of Solid State Chemistry*, vol. 178, pp. 831-846, 2005.